

Optimum performance of structural control with friction dampers

H. Caudana Quintana^{a,*}, M. Petkovski^b

^a Department of Structural Engineering, University of California, San Diego, La Jolla 92093, United States

^b Department of Civil and Structural Engineering, The University of Sheffield, Sheffield S1 3AJ, United Kingdom



ARTICLE INFO

Keywords:

Friction damper
Passive control
Semiactive control
Optimum control
Seismic retrofit

2010 MSC:

00-01

99-00

ABSTRACT

Friction-based structural control is an available strategy for reducing the seismic response of buildings. The friction dampers in such systems can be operated using passive and semiactive control. Passive dampers with constant, pre-defined capacity are effective and simple, but their adaptability to a broad range of frequency excitations is limited and their optimal configuration is complex. Semiactive control provides a means to vary the dampers' capacity to their optimum levels in real-time, but time delays in the control action may affect their performance. In this investigation, a passive system is initially introduced in a multi-storey steel frame to identify a threshold of optimum control force demand related to the limits of the building's elastic response. A new semiactive algorithm is then introduced to adjust the dampers' capacity based on the current deformation state across the building. From simulations of the non-linear response of the frame, the semiactive system reduced the structural response to levels similar to the optimum passive control, with more uniform distributions of storey drift. The control system had optimum performance when a range of time delays was included to simulate different regulator mechanisms.

1. Introduction

A mechanism for dissipation of the seismic energy exerted in buildings during strong earthquakes is through damage at specific locations in the structure. The damage, in the case of moment resistant frames, develops in the form of plastic hinges at the ends of beam elements. This may induce degradation of the structural resistance, with associated costs of repair and aesthetic degradation. As an alternative mechanism, passive and semiactive control systems are of particular interest due to their high energy dissipation capability. By using such systems, the dissipative capacity of the structure is increased, without modifying its original design strength.

An extensive description of control systems can be found in Housner et al. [1]. Symans et al. [2] give a good treatment of passive control and its applications, and Parulekar and Reddy [3] present the state-of-the-art of passive systems. Description of semiactive systems and examples of applications are described by Morales-Beltran et al. [4], Casciati et al. [5], Spencer and Nagarajaiah [6], Symans and Constantinou [7], and Spencer and Sain [8]. Amezcua-Fuentes et al. [9] present a review of control laws implemented in semiactive systems.

Passive control systems are activated by the action imposed by the main structural system. After the control device is installed, it has no ability to regulate itself under different ground motions. Control systems with frictional mechanisms (e.g., [10–14]) are simple and cost-

effective. However, the optimum performance of friction-based passive control is given by a unique configuration of slip-load capacity and placement of the dampers [15]. Filiatrault and Cherry [16] noted different performance between systems with slip-loads that were either proportional to the inter-storey shear force or uniformly distributed, and proposed a design slip-load spectrum to determine the optimum slip-load directly. Dowdell and Cherry [17] proposed a proportional distribution of the dampers' slip-load based on the structural deformation of the fundamental mode and the mass of the building. Apostolakis and Dargush [18] used genetic algorithms to identify the optimum capacity and placement of friction dampers in low-rise moment resistant steel frames. Min et al. [19] proposed the design of a single storey structure with friction damper based on a target equivalent damping ratio derived from the frictional hysteretic mechanism into a viscous damping mechanism at the steady-state response condition in the structure, which was subjected to harmonic ground motion. Lee et al. [20] studied the optimisation of damper capacity and allocation based on the normalisation of the ratio of slip-load to shear force in the building, either by considering the damper-braced frame or the bare frame, and proposed an empirical equation to determine the optimum quantity of dampers. Miguel et al. [21] studied the simultaneous optimisation of damper slip-load and placement by means of the backtracking search optimisation algorithm [22] with an objective function (e.g., maximum reduction of inter-storey drift for a shear

* Corresponding author.

E-mail address: hcaudanaquintana@eng.ucsd.edu (H. Caudana Quintana).

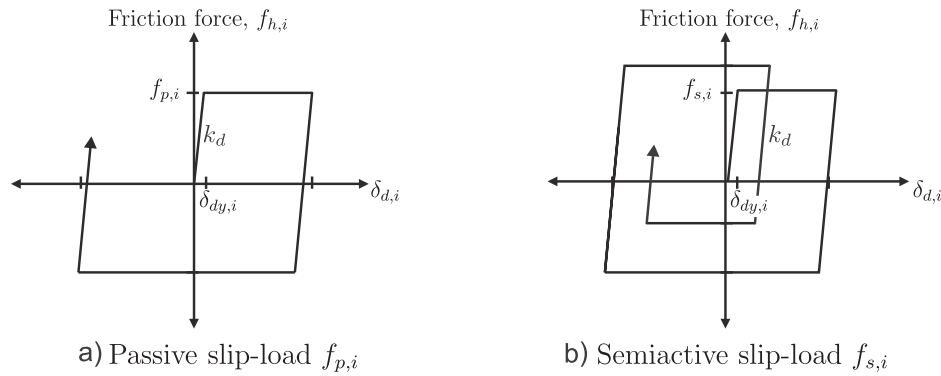


Fig. 1. Hysteretic behaviour of friction damper using different control schemes.

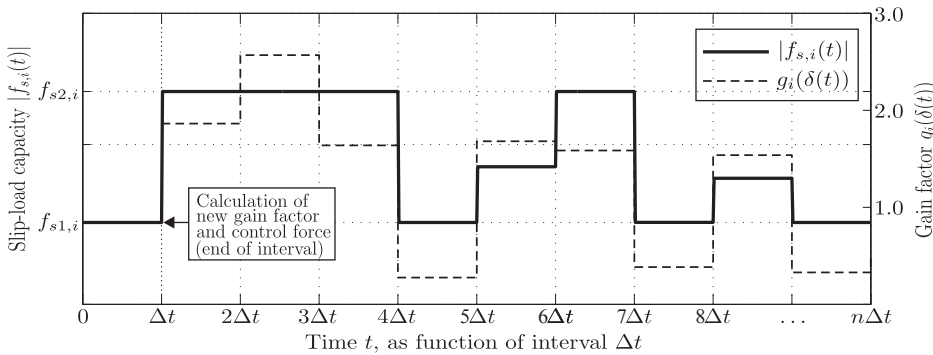


Fig. 2. Schematic functioning of $A\delta VG$ semiactive control.

building, or top displacement for a transmission line tower) and by feeding the optimisation algorithm only with the maximum capacity and placement of dampers available. For robust optimisation, Miguel et al. [23] introduced random variables to represent uncertainty in the material properties, ground motion and damper forces in each run of the backtracking search algorithm. From those studies, it can be concluded that the optimum passive slip-load is related to the characteristics of the earthquakes and thus, varies for different ground motions. Since it is tuned to a certain earthquake, the performance of passive systems may be affected for a broader range of excitation frequencies. Thus, rendering the design to sub-optimal performance as there is no way to predict ground motions. Furthermore, the optimisation process generally assumes an elastic structural response, which is non-realistic for design and maximum considered earthquakes.

Semiactive control is a possible solution to overcome the sub-optimal performance of passive dampers under different earthquakes. A semiactive control scheme is a means to manipulate the friction dampers in real-time during the earthquake to adjust the slip-loads to the most efficient level. The level of complexity and efficiency of the semiactive system depends on the control law implemented. Algorithms that require a full model of the structure may yield the best performance, but with an associated cost of implementation. Furthermore, the optimisation may be limited to elastic models of the structure. Algorithms that utilise a control architecture where minimal or no information is exchanged between each local controller are a compromise between good performance and fast computational response, but they may adapt more efficiently to non-linear response. Using the latter strategy, Akbay and Aktan [24] and Kannan et al. [25] proposed an algorithm based on bang-bang control to modify the slip-load of the so-called “active slip-bracing device” at fixed time and force increments. Dowdell and Cherry [17] developed an “off-on” control to modify the slip-load from a near-zero value (i.e., “off” phase) to a pre-set value (i.e., “on” phase). Inaudi [26] developed the modulated homogeneous control to modify the slip-load only at peaks of inter-storey deformation, and He et al. [27] enhanced this controller by introducing either

linear or hyperbolic tangent functions as boundary layer factors to allow smoother changes of the slip-load in the vicinity of motion reversal. Chen and Chen [28] developed an algorithm to include both viscous and Reid damping by defining different gain factors for the deformation phase and its rate. Ng and Xu [29] developed the non-sticking friction control to modify the slip-load up to a pre-defined maximum level proportionally to the hyperbolic tangent of the velocity. Ozbulut et al. [30] developed adaptive control algorithms using fuzzy logic to control friction dampers installed as supplemental devices for base isolated systems.

A possible drawback of the semiactive system is the unavoidable time lag that occurs during the feedback data acquisition, processing and transferring, and during the control force build-up in the control devices [31,32], which does not occur in passive systems.

In the investigation presented in this paper, a new semiactive control algorithm is introduced to modify the slip-loads based on the combination of local and global response parameters, which ensures adjustment of control forces based on knowledge of the whole building’s response without requiring a model of the full structure. The new algorithm increases the system’s adaptability to a variety of seismic excitations and eliminates the problem of optimum placement configuration by utilising a narrow range of control forces related to optimum passive slip-loads. The investigation of the effects of the time delays in the performance of the semiactive system is also presented.

2. Description of semiactive control algorithm

Modelling of the dynamic response of multi-degree-of-freedom (MDOF) structures with friction-based dissipation devices is given by Eq. (1) [33]:

$$M\ddot{x}(t) + C\dot{x}(t) + K(u)x(t) + F_h(t) = -ML\ddot{x}_g, \quad (1)$$

where M , C and $K(u)$ are the mass, damping and non-linear stiffness matrices, respectively; $x(t)$ is the vector of displacement relative to the ground and $\dot{}$ indicates derivative with respect to time; the input to the

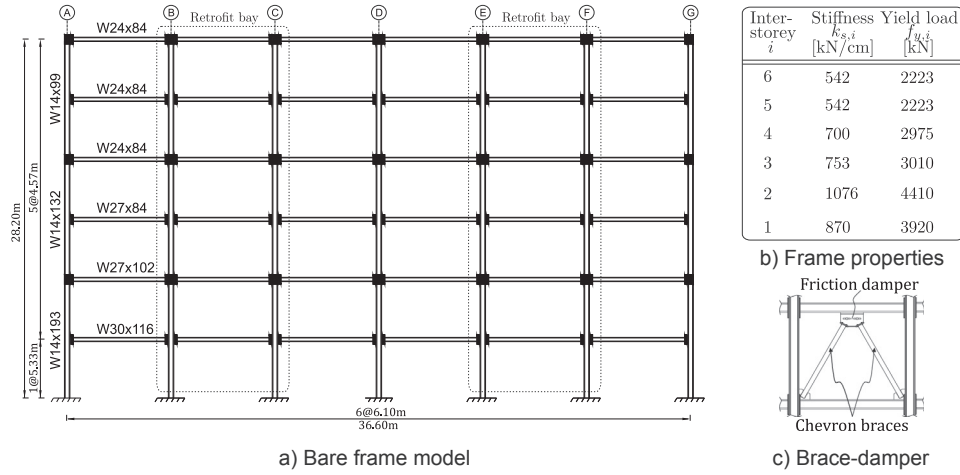


Fig. 3. Reference bare multi-storey frame.

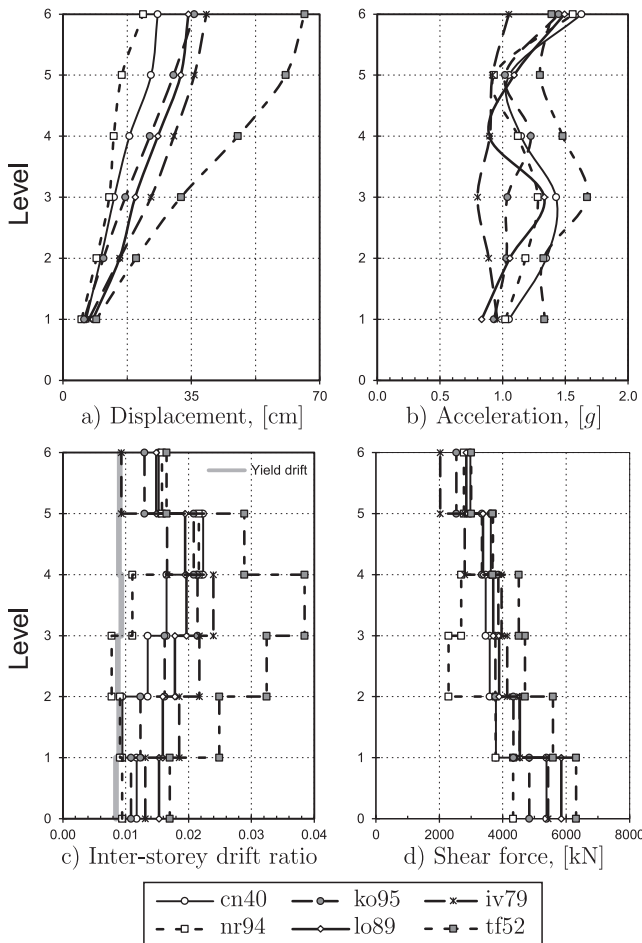


Fig. 4. Envelopes of absolute values of the bare frame's response.

system is the ground acceleration \ddot{x}_g , which is allocated to corresponding masses by the influence vector L . $F_h(t)$ is the vector of forces $f_{h,i}$ acting in each damper i . The force $f_{h,i}$ is given by the product of the damper's stiffness $k_{d,i}$ and the deformation $\delta_{d,i}$ in the damper before activation, and by the slip-load capacity at time of activation, i.e. when there is relative slippage at the frictional interface.

The slip-load capacity of friction dampers depends on the force clamping the moving parts together, and the friction coefficient in their interface. For passive dampers (Fig. 1a), the slip-load can be expressed as:

$$f_{p,i} = \mu N_i \text{sgn}(\dot{\delta}_{d,i}(t)), \quad (2)$$

where $f_{p,i}$ is the passive slip-load, N_i is the constant, pre-loaded clamping force, μ is the friction coefficient and $\text{sgn}(\dot{\delta}_{d,i}(t))$ indicates the direction of motion.

By introducing a controllable force application unit, it is possible to modify the damper's clamping force and slip-load in real-time using semiactive control. In this case, the semiactive slip-load $f_{s,i}(t)$ (Fig. 1b) is calculated as:

$$f_{s,i}(t) = \mu N_i(t) \text{sgn}(\dot{\delta}_{d,i}(t)), \quad (3)$$

where the force $N_i(t)$ is variable in time according to the semiactive control algorithm implemented.

In this investigation, the *Average Deformation with Variable Gain Factors* (A δ VG) algorithm is introduced to control the force $N_i(t)$ based on the actual state of the lateral deformation of the building. A variable gain factor $g_i(t)$ is introduced in the algorithm to calculate the required control force by combining local feedback (i.e. storey drift) and global information (i.e. the average value of all storeys' drift). In the algorithm, the clamping force $N_i(t)$ is adjusted only at pre-defined time intervals Δt (Fig. 2). Relatively long durations of Δt , based on the fundamental period of the structure, may preclude unnecessarily rapid operation of the adjusting mechanism and rattling in the dampers. Furthermore, the control operation would be closer to the frame's lower frequencies, where the largest response generally occurs.

At the end of each interval Δt , the gain factor $g_i(t)$ is calculated as a product of two components:

$$g_i(t) = g_{1,i}(t) \cdot g_{2,i}(t). \quad (4)$$

The first component is given by:

$$g_{1,i}(t) = \frac{|\hat{\delta}_i(t)|}{\frac{1}{n} \sum_{i=1}^n |\hat{\delta}_i(t)|}, \quad (5)$$

where $|\hat{\delta}_i(t)|$ is the absolute value of the largest drift of the i th inter-storey recorded within the interval Δt , and n is the number of storeys in the building. The role of this component is to produce a uniform distribution of inter-storey drifts along the height of the building by increasing or decreasing the slip-load proportionally to the ratio of the local storey drift to the mean value of drift in the building.

The second component was adapted from the smooth boundary layer algorithm [27] to gradually reduce the control force at the time of zero velocity (i.e. motion reversal and towards the end of excitation):

$$g_{2,i}(t) = \tanh(|\dot{\delta}_{d,i}(t)|), \quad (6)$$

where $\dot{\delta}_i(t)$ is the local velocity across the damper at the end of the

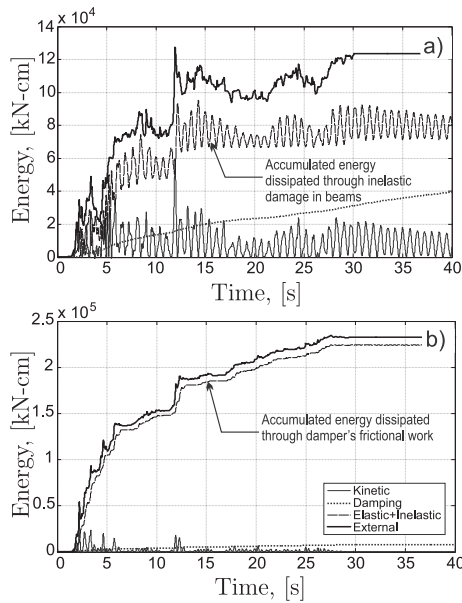


Fig. 5. Energy distribution for the El Centro earthquake: (a) Bare frame and (b) passive control, $f_{p,i} = 0.35f_y$.

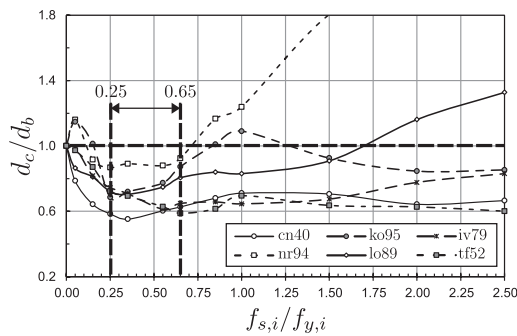


Fig. 6. Inter-storey drift ratio with passive control.

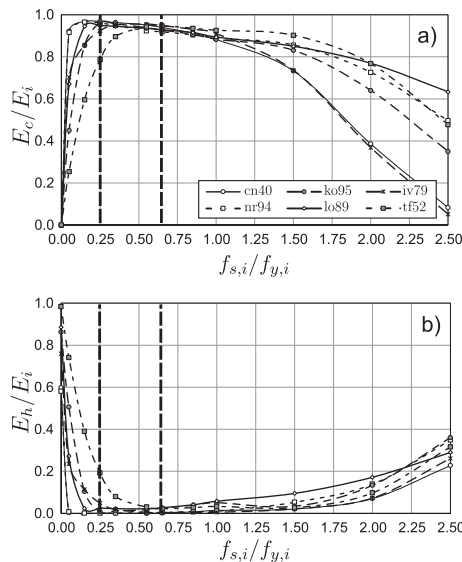


Fig. 7. Ratios of energy dissipated by (a) friction dampers and (b) plastic hinges in beams.

interval Δt .

The range of available clamping forces is capped to pre-defined minimum and maximum levels $N_{1,i}$ and $N_{2,i}$, respectively, which are related to the optimum range of passive slip-loads. Within these limits, the clamping force is adjusted by using the following equation:

$$N_i(t) = \begin{cases} N_{1,i} & \text{if } t \leq \Delta t \\ \max \left\{ \min \{g_i(t)|N_i(t-\Delta t)|; N_{2,i}\} \right\} & \text{if } m\Delta t < t \leq (m+1)\Delta t \end{cases} \quad (7)$$

where $m = 1, 2, 3, \dots, n$ (i.e. $m\Delta t$ is the time at the end of every interval of decision) and $N_i(t-\Delta t)$ is the clamping force determined in the previous interval of decision.

3. Reference frames

3.1. Bare model

The investigation was conducted by simulating the response of a low-rise steel frame in a purpose built software [34]. The six-storey, moment resistant frame (Fig. 3a) was first studied by Inaudi [26]. To create low damping conditions which were similar to the original frame, the proportional damping matrix C was constructed by using Rayleigh coefficients of 3.31×10^{-2} and 4.4×10^{-4} for the mass and initial stiffness matrices, respectively. The proportion of critical damping in the first, second and third mode resulted in 0.50%, 0.40% and 0.52%, respectively. The frame's first mode frequency was 0.67 Hz, second mode frequency was 1.88 Hz and third mode frequency was 3.16 Hz.

In order to determine appropriate levels of the control force related to the structural resistance, an initial pushover analysis of the bare frame was performed in Drain-2DX [35] by applying incremental lateral loads at each i th storey and monitoring the lateral deflection. The stiffness k_i and yield load $f_{y,i}$ are shown in Fig. 3b.

The response of the bare frame was simulated for six earthquake records: El Centro 1940 (cn40) recorded at IVI District Array #9, Northridge 1994 (nr94) recorded at LA-Fletcher Dr, Kobe 1995 (ko95) recorded at KJMA, Loma Prieta 1989 (lo89) recorded at San Francisco Bay Bridge, Imperial Valley 1979 (iv79) recorded at Calipatria Fire Station, and Taft 1952 (tf52) recorded at LA-Hollywood. The Pacific Earthquake Engineering Research [36] database records for each respective earthquake are 6, 993, 1106, 757, 163 and 12. All the records were scaled to peak ground acceleration $PGA = 0.55g$.

The Newmark's implicit average acceleration method was the algorithm used to integrate Eq. (1). Since the structure was modelled as an MDOF system with distributed mass and no DOF reduction, the time step for analysis was set as 5 ms. The hysteretic behaviour of the structure was simulated by means of plastic hinges representing the material non-linearity at both ends of the beam elements. The bilinear behaviour with post-yield softening was introduced by defining a post-yield to initial stiffness ratio of 5%. The moment resistance of the beams was determined as the product of the section's plastic modulus and the yield strength of steel grade S275. In order to generalise and satisfy the strong column-weak beam design typically required by seismic codes, which stipulate different ratios, (e.g., 1.3 for Eurocode 8 [37] and 1.0 for ASCE 7-10 [38]), the columns were modelled with elastic behaviour, regardless of their axial force-moment demand.

The envelope of the absolute values of displacement, acceleration, inter-storey drift ratio and shear force are shown in Fig. 4. For all the earthquakes, the frame had large incursions in the inelastic range (Fig. 4c), and the energy dissipated through the mechanism of plastic hinges in the beams accounted for more than half of the total energy exerted by the excitation (Fig. 5a).

Table 1
Indices J_1 to J_5 for assessment of control performance.

Parameter	Equation	Variables
Drift ratio	$J_1 = \left\{ \frac{\max(\delta_{c,i} /h_i)}{\max(\delta_{b,i} /h_i)} \right\}$	$\delta_{c,i}/h_i, \delta_{b,i}/h_i$ = Drift ratio at level i , for controlled and bare frame, respectively.
Acceleration	$J_2 = \left\{ \frac{\max \ddot{x}_{c,i} }{\max \ddot{x}_{b,i} } \right\}$	\ddot{x}_c, \ddot{x}_b = Acceleration relative to the ground.
Base shear	$J_3 = \left\{ \frac{\max F_{s,c} }{\max F_{s,b} } \right\}$	$F_{s,c}, F_{s,b}$ = Shear force at the base of the frame.
Average drift	$J_4 = \left\{ \frac{\max(\bar{\delta}_{c,i})}{\max(\bar{\delta}_{b,i})} \right\}$	$\bar{\delta}_{c,i}, \bar{\delta}_{b,i}$ = Average of simultaneous drift in the building at time of maximum drift of level i .
Drift distribution	$J_5 = \left\{ \frac{\max(\sigma_{c,i})}{\max(\sigma_{b,i})} \right\}$	$\sigma_{c,i}, \sigma_{b,i}$ = Standard deviation of drift across the building at time of maximum drift of level i .

3.2. Passive control system

The bare frame was initially retrofitted by introducing a concentric bracing-damper system in bays B-C and E-F at each storey (Fig. 3c). The braces consisted of steel, circular hollow sections designed to remain elastic and sufficiently stiff to allow relative slippage in the friction connections and avoid significant axial deformations. The dampers were modelled assuming frictional, slotted-bolted connections with rectangular hysteretic behaviour [11]. The combined passive slip-load $f_{p,i}$ for each pair of dampers at storey i was calculated as a function of the shear force resistance in the building, to reasonably correlate the control force with the actual resistance of the structure. The slip-loads were thus defined as a ratio of the bare frame yield load, i.e., $f_{p,i}/f_{y,i}$, varying from 0 to 2.5.

The ratios between controlled and bare frame’s maximum inter-

storey drift (d_c/d_b), with respect to the slip-load ratio $f_{p,i}/f_{y,i}$ are shown in Fig. 6. The optimum performance of the system varied for each earthquake, showing the limited adaptability of passive control. The range of slip-load ratios between 0.25 and 0.65 generally resulted in maximum reductions of the deformation, maximum levels of energy dissipated through the mechanism of frictional work in the connections and minimum levels of energy dissipated through damage in the beams (Fig. 7). Due to the inclusion of the control system, the damper’s frictional work acted as the main mechanism for energy dissipation (Fig. 5b). This additional dissipative capacity prevented any significant damage in the beams for the optimum range of $f_{p,i}$ between $0.25f_{y,i}$ and $0.65f_{y,i}$.

4. Performance of semiactive system

4.1. Control system with instantaneous action

In order to investigate the performance of the semiactive system, it is assumed that a mechanical regulator with instantaneous control action was available in each friction connection. The minimum and maximum levels of control force $N_{1,i}$ and $N_{2,i}$ were defined as $1.25f_{y,i}$ and $3.25f_{y,i}$, respectively. By using a friction coefficient $\mu = 0.2$, the resulting slip-loads are within the optimum range $0.25f_{y,i}$ to $0.65f_{y,i}$ identified for the passive control system. Three values for the interval of decision were defined as $\Delta t = T_f/4, T_f/2$ and T_f , where T_f is the fundamental period of the bare frame.

The performance of the control systems was measured in five different response parameters, as summarised in Table 1. The indices J_1 to J_5 reflect the performance of the passive and semiactive systems relatively to the response of the bare frame [39].

The time history of the slip-load (Fig. 8a) demonstrates the lower force levels required by the semiactive control for extended periods of time, which is advantageous to extend the durability of the dampers. As

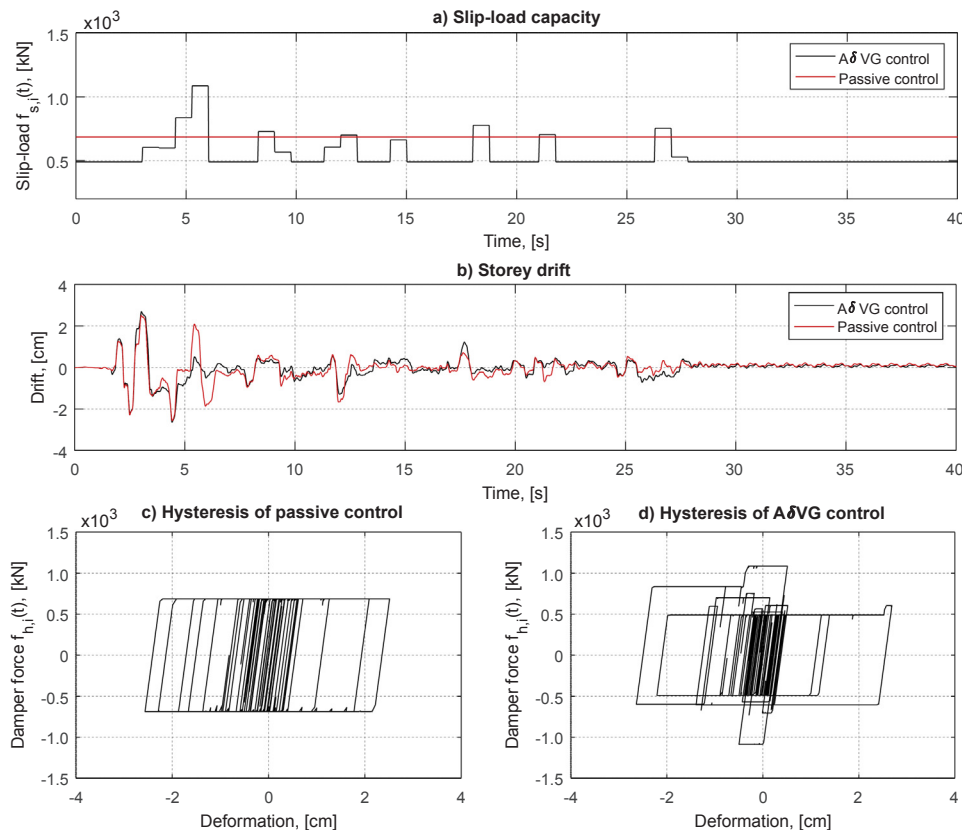


Fig. 8. Damper slip-load and frame response with optimum passive and semiactive control, under the El Centro 1940 earthquake.

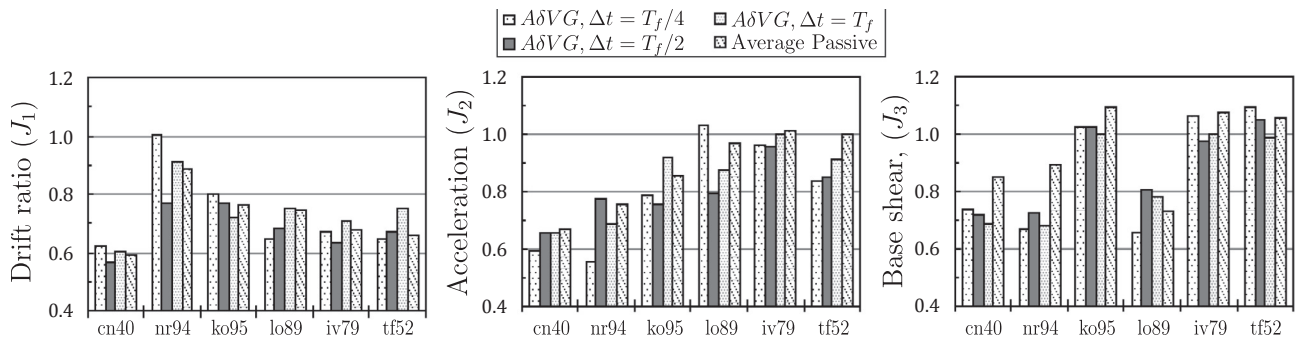


Fig. 9. Performance of the passive and semiactive control systems under different earthquakes.

Table 2
Average performance of the passive and semiactive control systems.

Response parameter	AδVG control, Δt=			Passive control, $f_p/f_y =$			
	$T_f/4$	$T_f/2$	T_f	0.25	0.35	0.65	Avg
Drift ratio \bar{J}_1	0.732	0.683	0.742	0.721	0.711	0.744	0.721
Acceleration \bar{J}_2	0.795	0.796	0.840	0.808	0.804	0.967	0.875
Base shear \bar{J}_3	0.872	0.881	0.855	0.794	0.871	1.104	0.948
Average drift \bar{J}_4	0.599	0.616	0.636	0.645	0.581	0.558	0.595
Drift distribution \bar{J}_5	0.397	0.382	0.445	0.439	0.404	0.448	0.430

shown in Fig. 8b, the frame with AδVG control had the same storey drift than the optimum passive control. However, the lower slip-loads in the semiactive system resulted in more frequent activation of the dampers. As the slip-load capacity increased, there were larger cycles of energy dissipation than the passive control (Fig. 8c and d).

4.1.1. Comparison of building response

The results from the simulations show that the semiactive control is efficient in reducing the structural response of the building for all the earthquakes. The system with shorter intervals (especially $\Delta t = T_f/2$) generally resulted in large reductions of storey drift, top floor acceleration and base shear, in comparison to the average optimum passive control for every earthquake (Fig. 9). The comparison of the average response for all earthquakes, with three cases of optimum passive slip-loads ($f_{p,i} = 0.25f_{y,i}, 0.35f_{y,i}, 0.65f_{y,i}$), the average response within the range $0.25f_{y,i}$ to $0.65f_{y,i}$ and the AδVG control is shown in Table 2. As shown in the Table, the semiactive system improved the frame’s response for drift, acceleration and shear force with lower indices \bar{J}_1, \bar{J}_2 and \bar{J}_3 calculated from the average response from all earthquakes.

4.1.2. Comparison of storey drift distribution

The semiactive system resulted in slightly lower drift reductions, but lower indices of standard deviation than the passive system. As shown in Fig. 10, the average simultaneous deformation levels indicated by the index J_4 are slightly lower for the average optimum passive system, approximately 6%, 5% and 10% for the Kobe, Loma Prieta and Imperial Valley earthquakes. For the El Centro, Northridge and Taft excitations,

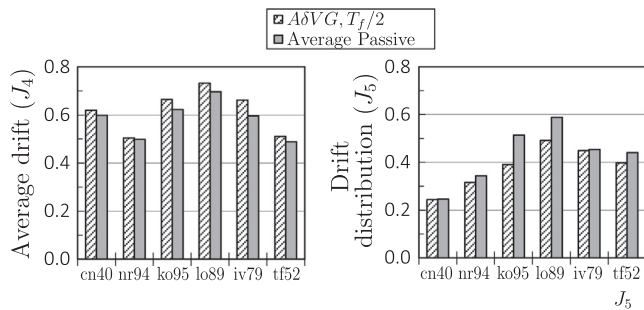


Fig. 10. Comparison of the average drift and their distribution for passive and semiactive control systems.

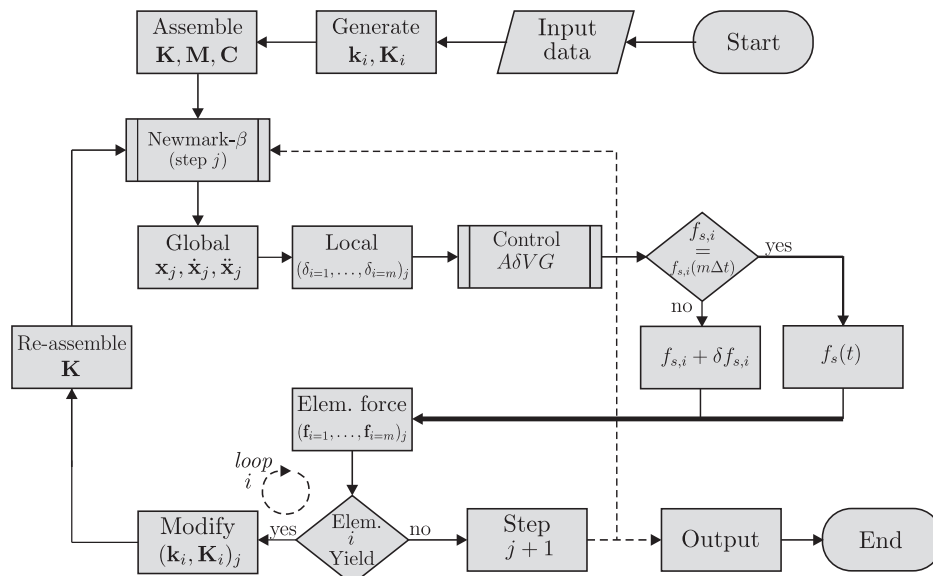


Fig. 11. Block diagram of analysis software with incremental substep in the control force.

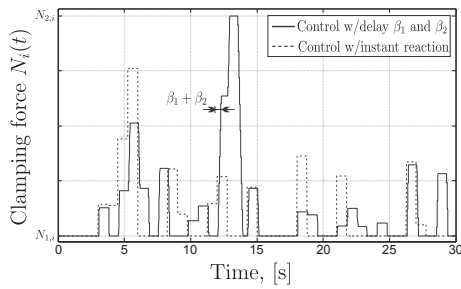


Fig. 12. Time history of semiactive clamping force.

however, the differences vary only between 1% and 3%.

In the case of the standard deviation of storey drift, the semiactive system resulted in values of J_5 that are 8%, 24%, 16% and 10% lower for Northridge, Kobe, Loma Prieta and Taft earthquakes. For the El Centro and Imperial Valley motions, the index levels are approximately 1% lower. For the combined response of all earthquakes (Table 2), the semiactive system with $\Delta t = T_f/2$ is 6% and 12% lower than the optimum passive case with $f_{p,i} = 0.35f_{y,i}$ and the average optimum passive range, respectively.

4.2. Control system with time delays

The time delays introduced in the simulations comprised two parts [31]: (i) fixed time delay β_1 due to acquisition, filtering, processing and

transmission of data in the cycle sensors-computers-actuators, and (ii) time delay β_2 that the actuators take to build up control forces, which in the case of friction dampers is associated with the mechanism used to adjust the clamping force $N_i(t)$, e.g. piezoelectric actuators [40–42], hydraulic actuators [25], electromagnetic fields [43,27], and brakes [44,45].

In this study, two series of simulations were performed using two values of the fixed time delay $\beta_1 = 30$ ms and 60 ms to cover the range of delays identified for magnetorheological damper tests [46]. In order to simulate the variety of possible clamping mechanisms in the friction dampers, the delay β_2 varied from 15 to 375 ms at intervals of 15 ms.

Due to the introduction of the delay β_1 , the semiactive control forces were determined at times $m\Delta t + \beta_1$ with the feedback information acquired at $m\Delta t$ (with $m = 1, 2, 3, \dots, n$). Thus, the factors $g_{1,i}$ and $g_{2,i}$ (Eqs. (5) and (6), respectively) were calculated as:

$$g_{1,i}(t) = \frac{|\hat{\delta}_i(t-\beta_1)|}{\frac{1}{n} \sum_{i=1}^n |\hat{\delta}_i(t-\beta_1)|}, \quad (8)$$

and

$$g_{2,i}(t) = \tanh(|\dot{\delta}_i(t-\beta_1)|). \quad (9)$$

To introduce the time delay β_2 between the command signals generated by the controller and the actual control action in the friction connections, the solution sequence in the analysis software was modified as shown in Fig. 11. An incremental approach based on the control action loading rate was defined as:

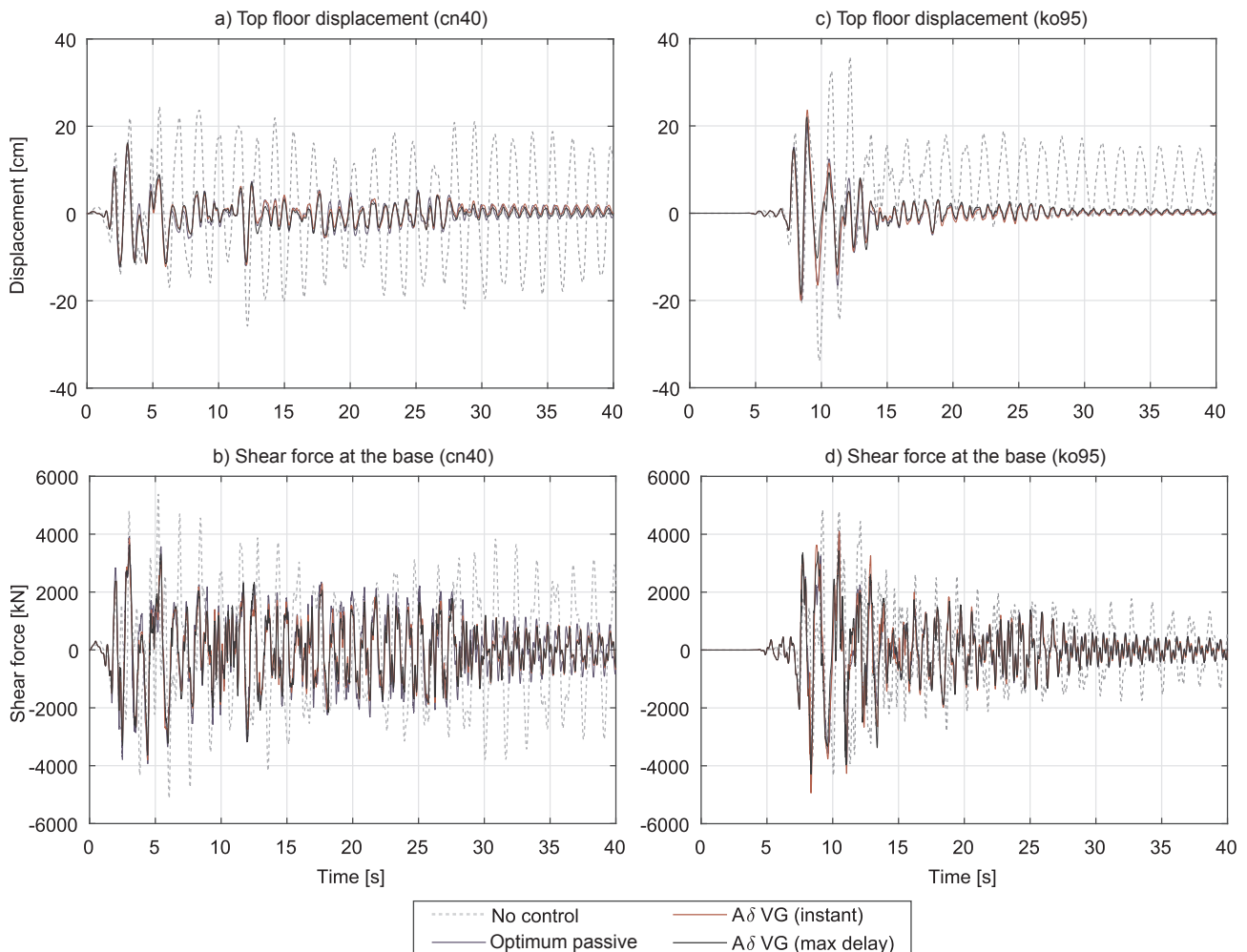


Fig. 13. Comparison of time histories for top floor displacement and shear force at the base.

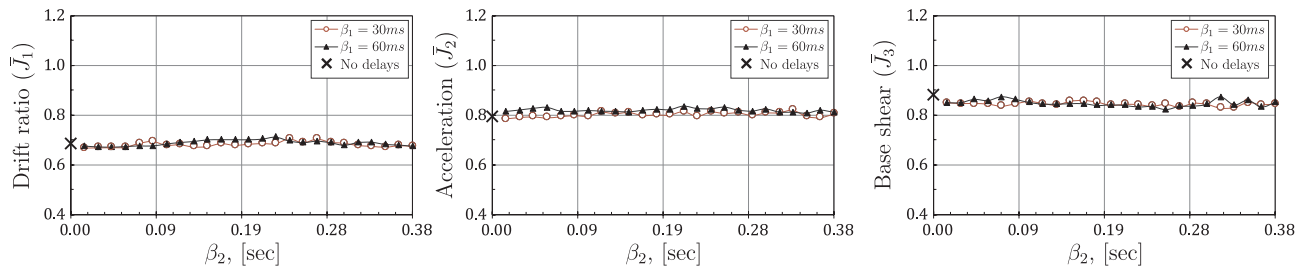


Fig. 14. Average performance of the semiactive system with instantaneous and delayed control action.

$$\delta N_i = \frac{\Delta N_i}{\beta_2} t_s, \quad (10)$$

where δN_i indicates the controllable force increment, ΔN_i is the available range of clamping force given by $N_{2,i} - N_{1,i}$. During the simulations, the clamping force was modified with the increment calculated with Eq. (10) using $t_s = 3dt$, due to the small integration time step $dt = 1/200$ s. Then, the modified slip-load capacity was calculated with Eq. (3) by adding or subtracting the increment δN_i to the current clamping force N_i , according to the sign of $f_{s,i}(m\Delta t) - f_{s,i}(t)$.

The effect of the time delay on the clamping force $N_i(t)$ in comparison to the system with no delays can be observed in Fig. 12. The system with delayed action generally resulted in a different control force demand than that of the system with instant response. For the time history shown, corresponding to the El Centro earthquake, the system with instant action required a lower peak control, which occurred at an earlier stage of the earthquake. The change in demand, however, does not necessarily mean activation in the damper, which rather depends on the deformation across its interface.

The introduction of the delays β_1 and β_2 did not affect significantly the performance of the control system in any of the simulation series. In comparison, the system with instantaneous action and the delayed system with longest delay $\beta_2 = 375$ ms under the El Centro and Imperial Valley earthquakes had maximum variations of 3.7%, 3.7% and 5.2% for the indices J_1 , J_2 and J_3 , respectively. In the case of Northridge, Loma Prieta and Taft earthquakes, the variations of the indices J_1 and J_3 were 8.8%, and 12%, respectively. The index J_2 was reduced by approximately 16.9% for Northridge, but slightly increased by 8.6% for the Loma Prieta excitation. In the case of Kobe earthquake, there was a gradual variation along the increase of the time delay, leading to reductions of approximately 20% for J_1 and 13% for J_3 , and an increase of 6% for J_2 . Time histories of the top floor displacement and base shear for the El Centro and Kobe earthquakes are shown in Fig. 13, for the cases of no control, optimum passive control, A δ VG with instantaneous control action and A δ VG with maximum delay.

The average indices \bar{J}_1 , \bar{J}_2 and \bar{J}_3 for the combined response of the six earthquakes are shown in Fig. 14. It is evident that there is not a significant influence of the time delay in the response. This is due to the fact that the friction damper is inherently a dissipative mechanism. Apparently, there is a balancing condition for the hysteretic dissipative areas depending on whether the command force is higher or lower than the current control force.

5. Conclusions

Passive friction dampers were used as initial retrofit solution for a low-rise moment resistant steel frame. The optimum performance varied for different capacity of the dampers and different ground motions. A threshold of control forces was identified for a set of six earthquake records scaled to the same PGA to provide similar levels of intensity, but different frequency content.

The A δ VG semiactive control was presented as a possible solution to the difficulty of finding the optimum configuration of passive dampers. The semiactive control allowed real-time variation of slip-loads based

on minimal feedback of the actual deformation state across the building. The comparison of the structural response with both control schemes demonstrated advantages of the semiactive system, including: (i) self-regulation that results in optimum performance when compared to passive control, (ii) increased adaptability to different ground excitations; (iii) narrow range of control force demand that is correlated with the actual resistance of the building, hence limiting excessive additional loads in structural elements; and (iv) more uniform distributions of inter-storey drift.

The numerical results, including time delays to simulate different regulator mechanisms showed a comparable performance for the system with and without delays.

Acknowledgements

The first author is grateful for the financial support provided by the National Council for Science and Technology of Mexico.

Appendix A. Supplementary material

Supplementary data associated with this article can be found, in the online version, at <http://dx.doi.org/10.1016/j.engstruct.2018.06.017>.

References

- [1] Housner GW, Bergman LA, Caughey TK, Chassiakos AG, Claus RO, Masri SF, Skelton RE, Soong TT, Spencer Jr. BF, Yao JTP. Structural control: past, present and future. *J Eng Mech - ASCE* 1997;123(9):897–971.
- [2] Symans MD, Charney FA, Whittaker AS, Constantinou MC, Kircher CA, Johnson MW, McNamara RJ. Energy dissipation systems for seismic applications: current practice and recent developments. *J Struct Eng - ASCE* 2008;134(1):3–21.
- [3] Parulekar Y, Reddy G. Passive response control systems for seismic response reduction: a state-of-the-art review. *Int J Struct Stab Dynam* 2009;9(1):151–77.
- [4] Morales-Beltran M, Paul J. Technical Note: active and semi-active strategies to control building structures under large earthquake motion. *J Earthq Eng* 2015;19(7):1086–111.
- [5] Casciati F, Magonette G, Marazzi F. Technology of semiactive devices and applications in vibration mitigation. Chichester (England): John Wiley & Sons, Ltd.; 2006.
- [6] Spencer Jr. BF, Nagarajaiah S. State of the art of structural control. *J Struct Eng - ASCE* 2003;129(7):845–56.
- [7] Symans MD, Constantinou MC. Semi-active control systems for seismic protection of structures: a state-of-the-art review. *Eng Struct* 1999;21(6):469–87.
- [8] Spencer Jr. BF, Sain MK. Controlling buildings: a new frontier in feedback. *IEEE Control Syst Magaz* 1997;17(6):19–35.
- [9] Amezcua-Sanchez JP, Dominguez-Gonzalez A, Sedaghati R, Romero-Troncoso R, Osornio-Rios RA. Vibration control on smart civil structures: a review. *Mech Adv Mater Struct* 2014;21(1):23–38.
- [10] Pall AS, Marsh C. Response of friction damped braced frames. *J Struct Div - ASCE* 1982;108(6):1313–23.
- [11] Grigorian CE, Yang TS, Popov EP. Slotted bolted connection energy dissipators. *Earthq Spectra* 1993;9(3):491–504.
- [12] Martinez-Rueda JE, Elnashai AS. A novel technique for the retrofitting of reinforced concrete structures. *Eng Struct* 1995;17(5):359–71.
- [13] Cho CG, Kwon M. Development and modeling of a frictional wall damper and its applications in reinforced concrete frame structures. *Earthq Eng Struct Dynam* 2004;33(7):821–38.
- [14] Martinelli P, Mulas MG. An innovative passive control technique for industrial precast frames. *Eng Struct* 2010;32(4):1123–32.
- [15] Pall AS, Pall RT. Performance-based design using Pall friction dampers - An economical design solution. In: 13th World conference on earthquake engineering, vol. 1955. Vancouver (BC, Canada); 2004.

- [16] Filiatrault A, Cherry S. Seismic design spectra for friction-damped structures. *J Struct Eng* 1990;116(5):1334–55.
- [17] Dowdell DJ, Cherry S. On passive and semi-active friction damping for seismic response control of structures. Eleventh world conference on earthquake engineering. Elsevier Science, Ltd.; 1996.
- [18] Apostolakis G, Dargush GF. Optimal seismic design of moment-resisting steel frames with hysteretic passive devices. *Earthq Eng Struct Dynam* 2010;39(4):355–76.
- [19] Min KW, Seong JY, Kim J. Simple design procedure of a friction damper for reducing seismic responses of a single-story structure. *Eng Struct* 2010;32(11):3539–47.
- [20] Lee SH, Park JH, Lee SK, Min KW. Allocation and slip load of friction dampers for a seismically excited building structure based on storey shear force distribution. *Eng Struct* 2008;30(4):930–40.
- [21] Miguel LFF, Miguel LFF, Lopez RH. Simultaneous optimization of force and placement of friction dampers under seismic loading. *Eng Optim* 2016;48(4):582–602.
- [22] Civicioglu P. Backtracking search optimization algorithm for numerical optimization problems. *Appl Math Comput* 2013;219(15):8121–44.
- [23] Miguel LFF, Miguel LFF, Lopez RH. Failure probability minimization of buildings through passive friction dampers. *Struct Des Tall Spec Build* 2016;25(17):869–85.
- [24] Akbay Z, Aktan HM. Intelligent energy dissipation devices. In: *Fourth U.S. national conference on earthquake engineering*, Vol. 3. California: Palm Springs; 1990. p. 427–35.
- [25] Kannan S, Uras H, Aktan H. Active control of building seismic response by energy dissipation. *Earthq Eng Struct Dynam* 1995;24(5):747–59.
- [26] Inaudi JA. Modulated homogeneous friction control: a semi-active damping strategy. *Earthq Eng Struct Dynam* 1997;26(3):361–76.
- [27] He WL, Agrawal AK, Yang JN. Novel semiactive friction controller for linear structures against earthquakes. *J Struct Eng* 2003;129(7):941–50.
- [28] Chen G, Chen C. Semiactive control of the 20-story benchmark building with piezoelectric friction dampers. *J Eng Mech - ASCE* 2004;130(4):393–400.
- [29] Ng CL, Xu YL. Semi-active control of a building complex with variable friction dampers. *Eng Struct* 2007;29(6):1209–25.
- [30] Ozbulut OE, Bitaraf M, Hurlebaus S. Adaptive control of base-isolated structures against near-field earthquakes using variable friction dampers. *Eng Struct* 2011;33(12):3143–54.
- [31] Agrawal AK, Yang JN. Effect of fixed time delay on stability and performance of actively controlled civil engineering structures. *Earthq Eng Struct Dynam* 1997;26(11):1169–85.
- [32] Datta TK. A state-of-the-art review on active control of structures. *ISET J Earth Technol* 2003;40(1):1–17.
- [33] Christopoulos C, Filiatrault A. Principles of passive supplemental damping and seismic isolation. Pavia: IUSS Press; 2006.
- [34] Caudana H. Semiactive friction connections for seismic control of multi-storey buildings, Ph.D. thesis. The University of Sheffield; 2013.
- [35] Prakash V, Powell G, Campbell S. Drain-2DX: Base program description and user guide, Version 1.10, Tech. Rep. Berkeley: University of California; 1993.
- [36] Pacific Earthquake Engineering Research Center, Strong Earthquake Database; 2011 < http://peer.berkeley.edu/peer_ground_motion_database > .
- [37] European Committee for Standardisation. Eurocode 8: Design of structures for earthquake resistance, Part 1: General rules, seismic actions and rules for buildings, BS EN1998-1:2004; 1998.
- [38] American Society of Civil Engineers. ASCE/SEI 7-10: Minimum design loads for buildings and other structures; 2013.
- [39] Ohtori Y, Christenson RE, Spencer Jr. BF, Dyke SJ. Benchmark control problems for seismically excited nonlinear buildings. *J Eng Mech* 2004;130(4):366–85.
- [40] Pardo-Varela JP, De la Llera JC. A semi-active piezoelectric friction damper. *Earthq Eng Struct Dynam* 2015;44(3):333–54.
- [41] Xu YL, Ng CL. Seismic protection of a building complex using variable friction damper: experimental investigation. *J Eng Mech - ASCE* 2008;134(8):637–49.
- [42] Unsal M, Niezrecki C, Crane III C. A new semi-active piezoelectric-based friction damper. In: *Smart structures and materials*, vol. 5052. International Society for Optics and Photonics; 2003. p. 413–20.
- [43] Amjadian M, Agrawal AK. A passive electromagnetic eddy current friction damper (PEMECFD): theoretical and analytical modeling. *Struct Control Health Monitor (e1978)* 2017:1–23.
- [44] Downey A, Cao L, Laflamme S, Taylor D, Ricles J. High capacity variable friction damper based on band brake technology. *Eng Struct* 2016;113:287–98.
- [45] Laflamme S, Taylor D, Abdellaoui Maane M, Connor JJ. Modified friction device for control of large-scale systems. *Struct Control Health Monitor* 2012;19(4):548–64.
- [46] Cha Y-J, Agrawal AK, Dyke SJ. Time delay effects on large-scale MR damper based semi-active control strategies. *Smart Mater Struct* 2013;22(1):1–13.